JOURNAL OF GUIDANCE, CONTROL, AND DYNAMICS
Vol. 25, No. 6, November–December 2002

Local Regularization of the Restricted Elliptic Three-Body Problem in Rotating Coordinates

Jean Albert Kechichian*
The Aerospace Corporation, El Segundo, California 90245-4691

The singular differential equations of motion of the restricted elliptic three-body problem in the sun–Earth L_1-centered rotating system are regularized to remove the singularity near the Earth center, thereby allowing the use of unconstrained optimization software in solving, through an iterative scheme, general transfer problems, including, for example, the transfer problem from a low circular parking orbit to any location in the vicinity of L_1. The trajectory is integrated backward from an arbitrarily selected point in space, and the maneuver velocity change components are searched to achieve certain target parameters at the closest approach to the Earth. Unlike the restricted circular problem, where use is made of the Jacobi constant to reduce the order of the differential system, the present restricted elliptic problem requires the addition of a differential equation for the energy variable, resulting in a system of ten first-order equations cast in terms of the well-known Levi-Civita–Kustaanheimo–Stiefel regularized u variables. As an example of a transfer from the Earth to a halo orbit around L_1, it is shown that the transfer solution obtained with the circular assumption fails to reach the desired halo-insertion location near L_1 when the trajectory is calculated within the framework of the more accurate elliptic model, thereby justifying the use of this latter model for higher-fidelity trajectory generation.

Introduction

THE control and use of libration-point satellites has benefited from the considerable contribution of Farquhar,[1] who successfully made use of the theory of the restricted circular and elliptic three-body problem thoroughly documented in Refs. 2–5. Another important contribution in generating periodic halo orbits in the circular problem using analytic models is attributed to Richardson.[6] He provides first- and third-order approximations to the crucial initial conditions that are later iterated on, in an exact sense, through numerical integration, to design a desired closed periodic halo path. These powerful methods are employed by Pernicka[7] and Hiday,[8] who tackled the more accurate elliptic model in determining various stationkeeping strategies and optimal transfers between libration-point orbits.

The regularization method devised by Levi-Civita,[9] Kustaanheimo,[10] and Kustaanheimo and Stiefel,[11] and thoroughly documented by Stiefel and Scheifele,[12] has been put to effective use by Howell and Breakwell[13] to study certain limiting cases of halo orbits. It was also used by Mains[14] to generate transfer trajectories from a low circular parking orbit around the Earth to the halo orbit of choice within the assumption of the circular problem. These and other similar computational techniques are further discussed[15] within the circular assumption and in terms of rotating coordinates centered at L_1, with effective removal of the singularity at the Earth's center. The circular problem, with the further restriction of maneuvering only in the ecliptic plane at halo insertion, is further analyzed[16] to establish the existence of economical families of transfer categories. The circular model is also used to determine the particular locations on the halo orbit to target to, such that the constrained insertion cost is further minimized. This present work shows the derivations that lead to the generation of a suitable set of first-order differential equations describing the three-dimensional motion of a spacecraft subject to the gravitational attraction of the sun and the Earth, which revolve in elliptic orbits around their moving barycenter. The singularity at the Earth's center is removed by regularizing these restricted elliptic three-body equations using rotating coordinates centered at the oscillating L_1 Lagrange point. Computer codes are then written using unconstrained minimization software, as are double-precision integrators with built-in interpolators for exacting calculations. An example of a transfer from a low Earth orbit to a particular point near L_1 is shown by iterating on two components of the insertion-velocity change, fully satisfying the required boundary constraints. The full three-dimensional search example requires only a minor modification of the codes. The mathematics of the regularization equations are shown in detail in the second section, and the mechanizations that produce the transfer are shown in the section following.

General Discussion

Dynamic systems theory has been put to effective use in the past decade to solve transfer problems from the Earth to the collinear L_1 and L_2 libration points[17,18] of the sun–Earth system, as well as the heteroclinic transfers[19] between these equilibrium points, with zero insertion cost in most cases. The stable and unstable invariant manifolds associated with a three-dimensional halo orbit, or with a planar Lyapunov orbit, asymptotically approach or depart from these orbits with zero insertion or ejection cost, respectively. For sufficiently large halo orbits, their invariant stable manifolds come very close to the Earth, thereby providing a natural path to transfer to these type of orbits with zero insertion cost.[17]

Although the numerical procedure used in this paper, as well as in Ref. 20, is based on backward integration starting at the halo fixed point, coupled with a differential correction scheme, the solutions obtained via the invariant manifolds also rely on backward integration and differential correction[21,22] to converge on a desired transfer that departs the Earth orbit from a given altitude.

The procedure that generates a stable manifold associated with a given fixed point on a given halo orbit[22] consists of selecting a new initial state, obtained via a small displacement, from the fixed point in the direction of the six-dimensional eigenvector associated with the stable eigenvalue of the monodromy matrix (the six-dimensional state-transition matrix whose time span is equal to one full period of the halo orbit). This state transition matrix corresponds to the linearized variational system, which, for halo orbits in the circular problem, has the real eigenvalues $\lambda_1 > 1$, $\lambda_2 = 1/\lambda_1$, and $\lambda_3 = \lambda_4 = 1$ and the complex eigenvalues $\lambda_5 = \lambda_6^*$, where the asterisk superscript indicates a complex conjugate. The stable eigenvector

Received 7 June 2001; presented as Paper 01-325 at the AAS/AIAA Astrodynamics Specialists Conference, Quebec, QC, Canada, 30 July–2 August 2001; revision received 17 June 2002; accepted for publication 17 July 2002.

*Engineering Specialist, Astrodynamics Department, Mail Stop M4/947, P.O. Box 92957, Los Angeles, CA 90009; Jean.A.Kechichian@aero.org. Associate Fellow AIAA.

that approximates locally the direction of the stable manifold corresponds to $\lambda_2 < 1$. The six-dimensional state vector of the fixed point X^H is, thus, displaced along the six-dimensional stable eigenvector Y^{W^s} to create the new initial state[22] $X_0^{W^s} = X^H + dY^{W^s}$ in the immediate vicinity of X^H, or the halo point. Here, d is of the order of 200 km (Ref. 23). $X_0^{W^s}$ is then an approximation of the state X_0 that lies exactly on the stable manifold, with $X_0^{W^s}$ being located nearby.

Backward and forward numerical integration in time of the system differential equations will produce the stable manifold that is a trajectory that may pass near the Earth. This procedure is called the globalization of the manifold.

Once the eigenvector $Y_0^{W^s}$ is known at a point at $t = t_0$ on a halo orbit, the eigenvectors corresponding to all other points are simply obtained from the propagation using the state transition matrix from t_0 to the times t_i of the other points[22] $Y_i^{W^s} = \Phi(t_i, t_0) Y_0^{W^s}$. A new initial point displaced by d is calculated for each such point using $Y_i^{W^s}$, and the corresponding manifold generated by backward integration of the system equations, creating the tubes[18] on which the trajectories twist and move.

After selecting several hundred points evenly spaced in time on a given halo orbit, and generating the corresponding stable manifolds, a transfer trajectory that passes to within a small distance of a required altitude target may be found. By the selection of such a candidate trajectory and by the adjustment of the value of d, an exact desired target altitude may be matched.[22] In an alternate manner, a differential correction scheme may be used by adjusting the velocities at $X_0^{W^s}$ without modifying the position components or adjusting d, as was done earlier, to match certain parameters at closest flyby of the Earth, such as, for example, a desired altitude.[22]

Finally, if the manifolds do not pass close to the Earth, the continuation method is used, whereas intermediate altitudes between the manifold closest approach altitude and the final desired altitude are selected as new targets, and the solution from each case are used as a starting guess for the generation of the nearby case until the final problem is solved.[22]

It is, therefore, quite natural to couple the invariant manifold approach with a differential correction scheme involving backward numerical integration of the system equations, such as the regularized elliptic system centered at L_1 developed hereafter, especially for trajectories to or from asymptotic orbits such as the halo orbits. However, the regularized system shown in this paper is not restricted to these specific applications, but can also be used in the general case[23] of three-dimensional motion and, for example, to find transfer trajectories to distant retrograde orbits.[24,25]

The linear stability analysis that leads to the construction of the local manifolds that wrap around periodic orbits is based on the circular three-body model because the halo orbits do not experience closure in the elliptic problem, and they must be stationkept at regular intervals. Solutions obtained through invariant manifolds provide a good initial guess, however, which is later iterated on with the use of a high-fidelity dynamic model for actual flight-path design.

The regularization of the elliptic problem is discussed in Ref. 2 for the two-dimensional case by way of complex variables, instead of the u variables of Kustaanheimo–Stiefel. Integration error estimates after n Runge–Kutta steps of the singular and regularized equations for two-body motion in elliptic orbit[2] show that the error growth is about 30 times less with the regularized system for circular orbits and more than 1000 times less for highly eccentric orbits ($e = 0.9$). It is for this reason that the integration of the regularized system is much faster because of the larger steps selected by the integrator, with the accuracy of the integration not being sensitive to e.

The numerical runs carried out later used a requested relative accuracy in all solution components of 10^{-12}. The minimization algorithm UNCMIN,[26] designed for the unconstrained minimization of a real-valued function $F(\boldsymbol{x})$ of n variables denoted by $\boldsymbol{x}$, is used. Only the function itself must be provided by the user to this algorithm, which is based on a general descent method and a quasi-Newton scheme.[26]

Because of the robustness of the solutions and the minimization algorithm, the differential equations of the transition matrix are not developed for simultaneous integration with the system equations. The 6×6 transition matrix $\Phi(t, t_0)$ obeys $\dot{\Phi}(t, t_0) = A(t)\Phi(t, t_0)$, where $A(t)$ emanates from the linearized state variational equations, $\delta\dot{\boldsymbol{x}}(t) = A(t)\delta\boldsymbol{x}(t)$, with $\boldsymbol{x}$ standing for the six-dimensional state vector. $A(t)$ involves in the singular system the partial derivatives of the pseudopotential $U = \frac{1}{2}(\dot{x}^2 + \dot{y}^2) + (1-\mu)/d + \mu/r$, with respect to x, y, z, where μ is the mass parameter derived hereafter, and where are d and r are the distances from the spacecraft to the larger and smaller bodies, respectively. The partials of U are singular in the original nonregularized system, thereby affecting the accuracy of the integration of $\dot{\Phi}$ near the Earth.

Finally, the addition of perturbations from a third massive body such as the moon, or from solar pressure, requires further analysis to cast the dynamics in regularized form to allow, for example, accurate lunar flybys for trajectory shaping. One possible approach consists of using several independent variables, as in the case of the multiple binary problem depicted in Ref. 23.

Locally Regularized Equations of Motion of the Restricted Elliptic Three-Body Problem in L_1-Centered Rotating System

The barycentric equations of motion of the restricted elliptic three-body problem in terms of the inertial coordinates ξ_o, η_o, and ζ_o, as well as the more convenient rotating coordinates ξ, η, and ζ, are fully derived in Ref. 1, as well as in publications such as Refs. 2–5. Figure 1 (Ref. 1) shows how the sun–Earth line P_1P_2 rotates around the ζ_o axis, referred to the barycenter at O with angular velocity $\dot{\theta}$, with the angle θ measured from the inertial direction ξ_o. The spacecraft with infinitesimal mass m with respect to the masses of the sun, m_1, and the Earth, m_2, is located at P, and the variable sun–Earth distance is denoted by R. Following the well-established nomenclature, $m_1 = 1-\mu$ and $m_2 = \mu$, with $\mu = m_2/(m_1+m_2)$ and $m_1 + m_2 = 1$. The average sun–Earth distance is set to 1, with this distance representing the astronomical unit (AU) $a = 1$ AU $= 1.495978714 \times 10^8$ km, such that the mean angular velocity of the sun–Earth line, which also represents the mean motion of the Earth $n_E = 1.990986606 \times 10^{-7}$ rad/s, is also set to the unit value. When $M = n_E(t - \tau^*)$ designates the mean anomaly of the earth in its elliptic orbit of eccentricity e, with $t = \tau^*$ defining perigee, then R can be written in powers of the eccentricity[1]

$$R/a = 1 - ec_M - \tfrac{1}{2}e^2(c_{2M} - 1) - \tfrac{3}{8}e^3(c_{3M} - c_M), \ldots$$

and θ^*, the true anomaly, as

$$\theta^* = M + 2es_M + \tfrac{5}{4}e^2 s_{2M} + (e^3/12)(13s_{3M} - 3s_M), \ldots$$

Here, s_M and c_M stand for $\sin M$ and $\cos M$, respectively, etc.

From $\theta = \omega + \theta^*$, where ω is the argument of perigee, $\dot{\theta} = \dot{\theta}^* = (\mathrm{d}\theta^*/\mathrm{d}M)\dot{M}$ with $\dot{M} = n_E = 1$, such that $\dot{\theta} = 1 + 2ec_M + \frac{5}{2}e^2 c_{2M}$ and[1]

$$\dot{\theta} = 1 + \nu = 1 + 2e\cos(t - \tau^*) + \tfrac{5}{2}e^2\cos 2(t - \tau^*), \ldots$$

$$R = 1 + \rho = 1 - e\cos(t - \tau^*) - (e^2/2)[\cos 2(t - \tau^*) - 1)] + \cdots$$

The equations of motion in terms of the rotating coordinates x, y, and z attached to the libration point at L_1 have been derived in Ref. 1 using the Lagrangian formalism. They involve the quantities $\dot{\theta} = 1 + \nu$ and $\ddot{\theta} = \dot{\nu}$, which are explicit functions of time

$$\begin{aligned}\ddot{x} = {} & 2(1+\nu)\dot{y} - (1-\gamma_L)\ddot{\rho} + \dot{\nu}y + (1+\nu)^2[(1-\gamma_L)(1+\rho) + x] \\ & - \left[(1-\mu)\big/r_1^3\right][(1-\gamma_L)(1+\rho) + x] \\ & + \left(\mu\big/r_2^3\right)[\gamma_L(1+\rho) - x] - \mu/(1+\rho)^2 \end{aligned} \tag{1}$$

$$\begin{aligned}\ddot{y} = {} & -2(1+\nu)[(1-\gamma_L)\dot{\rho} + \dot{x}] - \dot{\nu}[(1-\gamma_L)(1+\rho) + x] \\ & + (1+\nu)^2 y - \left[(1-\mu)\big/r_1^3\right]y - \left(\mu\big/r_2^3\right)y \end{aligned} \tag{2}$$

$$\ddot{z} = -\left[(1-\mu)\big/r_1^3\right]z - \left(\mu\big/r_2^3\right)z \tag{3}$$

The varying distance between L_1 and the Earth is given by $\gamma_L R$, as shown in Fig. 2, with $\gamma_L = R_1/a$ and $R_1 = 1.497610042 \times 10^6$ km being the L_1–Earth distance in the circular problem. The distances r_1 and r_2 are given by $r_1 = \{[(1-\gamma_L)(1+\rho) + x]^2 + y^2 + z^2\}^{1/2}$ and

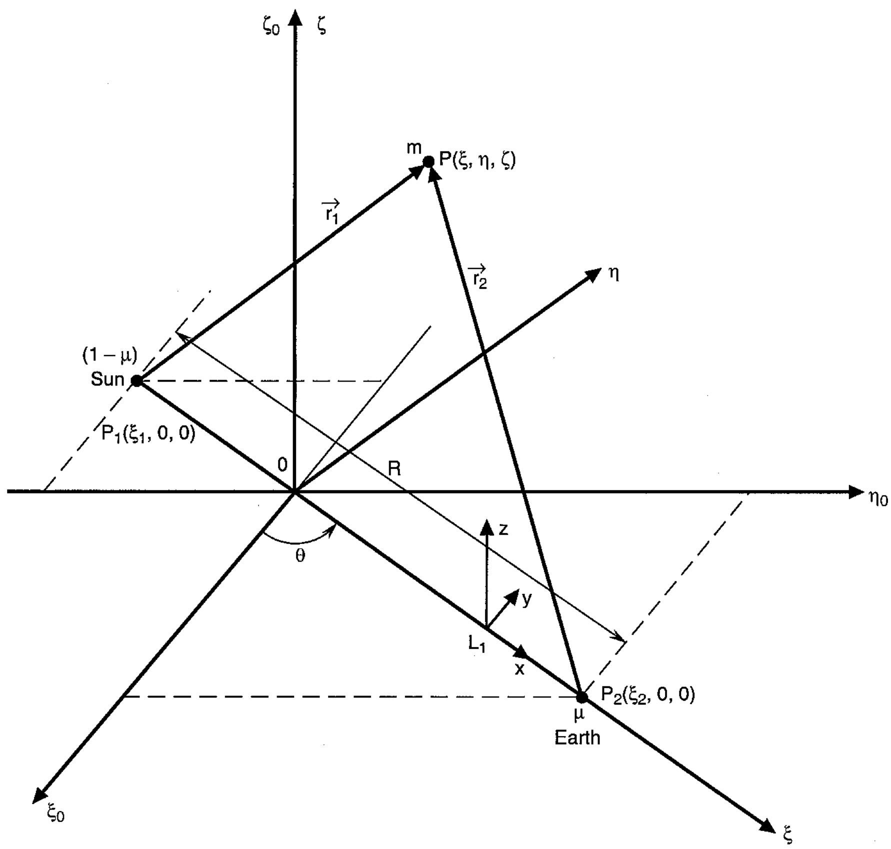

Fig. 1 Inertial and rotating axes.[1]

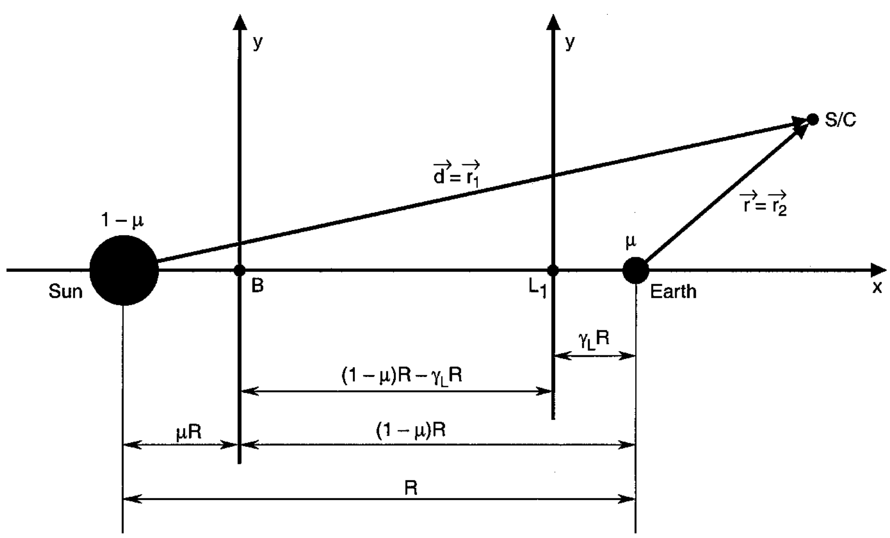

Fig. 2 Lagrange point and barycenter geometry.

$r_2 = \{[\gamma_L(1+\rho) - x]^2 + y^2 + z^2\}^{1/2}$, where x, y, and z are dimensionless quantities, and the derivatives are with respect to the nondimensional time $\tau'' = n_E t$. The angle θ is equal to zero when the two masses m_1 and m_2 are at their periapse and m_1 and m_2 orbit their barycenter in similarly oriented ellipses having a common eccentricity, with the common period of mean motion equaling n_E, but with different semimajor axes given by $a_1 = [m_2/(m_1+m_2)]a$ and $a_2 = [m_1/(m_1+m_2)]a$. In nondimensional form, $R = (1 - ec_E)$ with $e = 0.0167217$ also being the eccentricity of the orbit of m_2, the Earth, relative to m_1, the sun.

The variable angular rate $\dot{\theta}$ is given by

$$\dot{\theta} = \frac{h}{R^2} = \frac{\left[G(m_1+m_2)a(1-e^2)\right]^{\frac{1}{2}}}{a^2(1-ec_E)^2}$$

or, in nondimensional form,

$$\dot{\theta} = \frac{(1-e^2)^{\frac{1}{2}}}{(1-ec_E)^2} \tag{4}$$

because G, the universal gravitational constant, is also equal to the unit value because n_E was normalized to one. Here, h is the angular momentum of the two orbiting massive bodies, and E stands for the eccentric anomaly associated with the relative orbit of the Earth. The quantities $\dot{R}$, $\ddot{R}$, and $\ddot{\theta}$ needed in Eqs. (1–3) are obtained from the orbit equation and Eq. (4) in nondimensional form. Thus, $\dot{R} = \mathrm{d}R/\mathrm{d}\tau'' = es_E\dot{E}$, $\ddot{\theta} = (\mathrm{d}\dot{\theta}/\mathrm{d}E)\dot{E}$, and $\ddot{R} = ec_E\dot{E}^2 + es_E\ddot{E}$, with $\dot{E} = 1/(1-ec_E)$ and $\ddot{E} = -es_E\dot{E}^2/(1-ec_E)$ such that

$$\dot{R} = \frac{es_E}{(1-ec_E)} \tag{5}$$

$$\ddot{R} = \frac{ec_E - e^2}{(1-ec_E)^3} \tag{6}$$

$$\ddot{\theta} = \frac{-2es_E(1-e^2)^{\frac{1}{2}}}{(1-ec_E)^4} \tag{7}$$

Equations (1–3) can now be written in terms of the eccentric anomaly E as

$$\ddot{x} = \frac{2(1-e^2)^{\frac{1}{2}}}{(1-ec_E)^2}\dot{y} - (1-\gamma_L)\frac{\left(ec_E - e^2\right)}{(1-ec_E)^3} - \frac{2es_E(1-e^2)^{\frac{1}{2}}}{(1-ec_E)^4}y + \frac{(1-e^2)[(1-\gamma_L)(1-ec_E)+x]}{(1-ec_E)^4} - \frac{(1-\mu)}{r_1^3}[(1-\gamma_L)(1-ec_E)+x] + \frac{\mu}{r_2^3}[\gamma_L(1-ec_E)-x] - \frac{\mu}{(1-ec_E)^2} \tag{8}$$

$$\ddot{y} = -\frac{2(1-e^2)^{\frac{1}{2}}}{(1-ec_E)^2}\left[(1-\gamma_L)\frac{es_E}{(1-ec_E)} + \dot{x}\right] + \frac{2es_E(1-e^2)^{\frac{1}{2}}}{(1-ec_E)^4}[(1-\gamma_L)(1-ec_E)+x] + \frac{(1-e^2)}{(1-ec_E)^4}y - \frac{(1-\mu)}{r_1^3}y - \frac{\mu}{r_2^3}y \tag{9}$$

$$\ddot{z} = -\frac{(1-\mu)}{r_1^3}z - \frac{\mu}{r_2^3}z \tag{10}$$

where

$$r_1 = \left\{[(1-\gamma_L)(1-ec_E)+x]^2 + y^2 + z^2\right\}^{\frac{1}{2}} \tag{11}$$

$$r_2 = \left\{[\gamma_L(1-ec_E)-x]^2 + y^2 + z^2\right\}^{\frac{1}{2}} \tag{12}$$

These equations can be cast in a form where the derivatives are with respect to the physical time t by using $\mathrm{d}x/\mathrm{d}\tau'' = (1/n_E)(\mathrm{d}x/\mathrm{d}t)$, $\mathrm{d}^2x/\mathrm{d}\tau''^2 = (1/n_E^2)(\mathrm{d}^2x/\mathrm{d}t^2)$, etc.,

$$\ddot{x} = \frac{\mathrm{d}^2x}{\mathrm{d}t^2} = 2n_E b\dot{y} - (1-\gamma_L)cn_E^2 + dn_E^2 y + b^2[(1-\gamma_L)g + x]n_E^2 - \frac{(1-\mu)}{r_1^3}[(1-\gamma_L)g+x]n_E^2 + \frac{\mu}{r_2^3}(\gamma_L g - x)n_E^2 - \frac{\mu}{g^2}n_E^2 \tag{13}$$

$$\ddot{y} = -2b[(1-\gamma_L)kn_E^2 + n_E\dot{x}] - d[(1-\gamma_L)g+x]n_E^2 + b^2n_E^2y - \frac{(1-\mu)}{r_1^3}n_E^2y - \frac{\mu}{r_2^3}n_E^2y \tag{14}$$

$$\ddot{z} = -\frac{(1-\mu)}{r_1^3}n_E^2z - \frac{\mu}{r_2^3}n_E^2z \tag{15}$$

where x, y, and z are still dimensionless quantities, and the various coefficients appearing in the preceding differential equations are given as

$$b = \dot{\theta} = \frac{(1-e^2)^{\frac{1}{2}}}{(1-ec_E)^2}, \qquad c = \ddot{R} = \frac{\left(ec_E - e^2\right)}{(1-ec_E)^3}$$

$$d = \ddot{\theta} = -\frac{2es_E(1-e^2)^{\frac{1}{2}}}{(1-ec_E)^4}, \qquad g = R = (1-ec_E)$$

$$k = \dot{R} = \frac{es_E}{(1-ec_E)}$$

The circular restricted three-body equations of motion referred to the L_1 point[15] are readily recovered from Eqs. (13–15) by setting $e = 0$:

$$\ddot{x} = 2n_E\dot{y} + (1-\gamma_L)n_E^2 + n_E^2x - \left[(1-\mu)/r_1^3\right][(1-\gamma_L)+x]n_E^2 + \left(\mu/r_2^3\right)(\gamma_L - x)n_E^2 - \mu n_E^2$$

$$\ddot{y} = -2n_E\dot{x} + yn_E^2 - \left[(1-\mu)/r_1^3\right]n_E^2y - \left(\mu/r_2^3\right)n_E^2y$$

$$\ddot{z} = -\left[(1-\mu)/r_1^3\right]n_E^2z - \left(\mu/r_2^3\right)n_E^2z$$

with

$$r_1 = \left\{[(1-\gamma_L)+x]^2 + y^2 + z^2\right\}^{\frac{1}{2}}$$

$$r_2 = \left[(x-\gamma_L)^2 + y^2 + z^2\right]^{\frac{1}{2}}$$

The change of variable $\mathrm{d}t = r_2\,\mathrm{d}\tau$ is now used as the first step in regularizing the three differential equations (13–15) to remove the singularity at $r_2 = 0$, or, in practice, at closest approach to Earth's center. Because r_2'/r_2^3 is equivalent to $\boldsymbol{r}_2\cdot\boldsymbol{r}_2'/r_2^4$, with the prime standing for differentiation with respect to τ, and by the use of $\dot{x} = x'/r_2$, $\ddot{x} = -r_2'x'/r_2^3 + 1/r_2^2x''$, etc., the following form is obtained:

$$x'' = 2n_Ebr_2y' + \left(x'/r_2^2\right)(\boldsymbol{r}_2\cdot\boldsymbol{r}_2') + (\mu/r_2)(\gamma_Lg - x)n_E^2 + r_2^2\left\{-(1-\gamma_L)cn_E^2 + dn_E^2y + b^2[(1-\gamma_L)g+x]n_E^2 - \left[(1-\mu)/r_1^3\right][(1-\gamma_L)g+x]n_E^2 - \mu n_E^2/g^2\right\} \tag{16}$$

with

$$\boldsymbol{r}_2 = \{[-\gamma_LR + x]\;y\;z\}^T, \qquad \boldsymbol{r}_2' = \{[-\gamma_LR' + x']\;y'\;z'\}^T$$

and where

$$R' = \frac{\mathrm{d}R}{\mathrm{d}\tau} = \frac{\mathrm{d}R}{\mathrm{d}\tau''}\frac{\mathrm{d}\tau''}{\mathrm{d}t}\cdot\frac{\mathrm{d}t}{\mathrm{d}\tau} = kn_Er_2$$

$$\boldsymbol{r}_2\cdot\boldsymbol{r}_2' = (-\gamma_Lg + x)(-\gamma_Lkn_Er_2 + x') + yy' + zz'$$

Similarly,

$$y'' = -2bn_Er_2x' + \left(y'/r_2^2\right)(\boldsymbol{r}_2\cdot\boldsymbol{r}_2') - (\mu/r_2)n_E^2y + r_2^2\left\{b^2n_E^2y - \left[(1-\mu)/r_1^3\right]n_E^2y - 2b(1-\gamma_L)kn_E^2 - d[(1-\gamma_L)g+x]n_E^2\right\} \tag{17}$$

$$z'' = \left(z'/r_2^2\right)(\boldsymbol{r}_2\cdot\boldsymbol{r}_2') - (\mu/r_2)n_E^2z + r_2^2\left\{-\left[(1-\mu)/r_1^3\right]n_E^2z\right\} \tag{18}$$

When $x^* = x - \gamma_LR$, then $x^{*\prime} = x' - \gamma_Lkn_Er_2$ and $x^{*\prime\prime} = x'' - \gamma_L(cn_E^2r_2^2 + kn_Er_2')$ because $\mathrm{d}R/\mathrm{d}\tau'' = k$ and $\mathrm{d}^2R/\mathrm{d}\tau''^2 = c$, as derived earlier. Here, x^* is the value of x measured from the Earth's center and not from L_1. When the nomenclature used in the literature is followed and when

$$\boldsymbol{R}^* = (x^*, y, z, 0)^T, \qquad \boldsymbol{R}^{*\prime} = (x^{*\prime}, y', z', 0)^T$$

$$\boldsymbol{R}^{*\prime\prime} = (x^{*\prime\prime}, y'', z'', 0)^T$$

Eqs. (16–18) are transformed to the form involving the x^*, y, and z instead of the x, y, and z variables

$$x^{*\prime\prime} = 2n_Ebr_2y' + \left(x^{*\prime}/r_2^2\right)(\boldsymbol{r}_2\cdot\boldsymbol{r}_2') - (\mu/r_2)n_E^2x^* + r_2^2F_1^{**} \tag{19}$$

$$y'' = -2bn_Er_2x^{*\prime} + \left(y'/r_2^2\right)(\boldsymbol{r}_2\cdot\boldsymbol{r}_2') - (\mu/r_2)n_E^2y + r_2^2F_2^{**} \tag{20}$$

$$z'' = \left(z'/r_2^2\right)(\boldsymbol{r}_2\cdot\boldsymbol{r}_2') - (\mu/r_2)n_E^2z + r_2^2F_3^{**} \tag{21}$$

where the derivatives are with respect to τ and where the forcing functions are given by

$$F_1^{**} = -cn_E^2 + dn_E^2y + b^2(g + x^*)n_E^2 - \left[(1-\mu)/r_1^3\right](g + x^*)n_E^2 - (\mu/g^2)n_E^2 \tag{22}$$

$$F_2^{**} = b^2n_E^2y - \left[(1-\mu)/r_1^3\right]n_E^2y - 2bkn_E^2 - d(g + x^*)n_E^2 \tag{23}$$

$$F_3^{**} = -\left[(1-\mu)/r_1^3\right]n_E^2z \tag{24}$$

where x^*, y, and z are, of course, still dimensionless. The restricted circular three-body equations in terms of the L_1-centered x, y, and z variables are readily recovered by setting $e = 0$ in Eqs. (19–24), which are otherwise written in terms of x^*, y, and z:

$$x'' = 2n_E r_2 y' + \left(x'/r_2^2\right)(\boldsymbol{r}_2 \cdot \boldsymbol{r}_2') + (\mu/r_2)(\gamma_L - x)n_E^2 + r_2^2\left\{(1-\gamma_L)n_E^2 + n_E^2 x - \left[(1-\mu)/r_1^3\right] \times [(1-\gamma_L)+x]n_E^2 - \mu n_E^2\right\}$$

$$y'' = -2n_E r_2 x' + \left(y'/r_2^2\right)(\boldsymbol{r}_2 \cdot \boldsymbol{r}_2') - (\mu/r_2)n_E^2 y + r_2^2\left\{y n_E^2 - \left[(1-\mu)/r_1^3\right]n_E^2 y\right\}$$

$$z'' = \left(z'/r_2^2\right)(\boldsymbol{r}_2 \cdot \boldsymbol{r}_2') - (\mu/r_2)n_E^2 z + r_2^2\left\{-\left[(1-\mu)/r_1^3\right]n_E^2 z\right\}$$

where

$$\boldsymbol{r}_2 \cdot \boldsymbol{r}_2' = -(\gamma_L - x)x' + yy' + zz'$$

because in the circular case,

$$\boldsymbol{r}_2 = [(-\gamma_L + x), y, z]^T, \qquad \boldsymbol{r}_2' = (x', y', z')^T$$

The forcing functions also reduce to the form in Ref. 15:

$$F_1^* = (1-\gamma_L)n_E^2 + n_E^2 x - \left[(1-\mu)/r_1^3\right] \times [(1-\gamma_L)+x]n_E^2 - \mu n_E^2$$

$$F_2^* = y n_E^2 - \left[(1-\mu)/r_1^3\right]n_E^2 y, \qquad F_3^* = -\left[(1-\mu)/r_1^3\right]n_E^2 z$$

Equations (19–21) are equivalent to the vector differential equation

$$\boldsymbol{R}^{*\prime\prime} = [(\boldsymbol{R}^* \cdot \boldsymbol{R}^{*\prime})/(\boldsymbol{R}^* \cdot \boldsymbol{R}^*)]\boldsymbol{R}^{*\prime} + b n_E R^* B \boldsymbol{R}^{*\prime} - n_E^2 \mu(\boldsymbol{R}^*/R^*) + R^{*2}\boldsymbol{F}^{**} \tag{25}$$

where $R^* = |\boldsymbol{R}^*|$, $\boldsymbol{F}^{**} = (F_1^{**}, F_2^{**}, F_3^{**}, 0)^T$, and the matrix B is given by

$$B = \begin{bmatrix} 0 & 2 & 0 & 0 \\ -2 & 0 & 0 & 0 \\ 0 & 0 & 0 & 0 \\ 0 & 0 & 0 & 0 \end{bmatrix}$$

When $\bar{\bar{B}} = b n_E B$ and $\bar{\mu} = n_E^2 \mu$, Eq. (25) can be written as

$$\boldsymbol{R}^{*\prime\prime} = [(\boldsymbol{R}^* \cdot \boldsymbol{R}^{*\prime})/(\boldsymbol{R}^* \cdot \boldsymbol{R}^*)]\boldsymbol{R}^{*\prime} + R^* \bar{\bar{B}} \boldsymbol{R}^{*\prime} - \bar{\mu}(\boldsymbol{R}^*/R^*) + R^{*2} F^{**} \tag{26}$$

The second and third terms in the right-hand side of this equation represent Coriolis and Earth gravity acceleration terms, respectively. The Kustaanheimo–Stiefel transformation (see Refs. 10–12) $\boldsymbol{R}^* = L(\boldsymbol{u})\boldsymbol{u}$ is applied next, with

$$L(\boldsymbol{u}) = \begin{bmatrix} u_1 & -u_2 & -u_3 & u_4 \\ u_2 & u_1 & -u_4 & -u_3 \\ u_3 & u_4 & u_1 & u_2 \\ u_4 & -u_3 & u_2 & -u_1 \end{bmatrix}$$

Equation (26) is transformed to the u language by using $R^* = \boldsymbol{u} \cdot \boldsymbol{u}$, $\boldsymbol{R}^{*\prime} = 2L(\boldsymbol{u})\boldsymbol{u}'$, $\dot{\boldsymbol{R}}^* = \boldsymbol{R}^{*\prime}/R^*$, and

$$\bar{h} = \frac{\dot{\boldsymbol{R}}^* \cdot \dot{\boldsymbol{R}}^*}{2} - \frac{\bar{\mu}}{R^*} = \frac{2(\boldsymbol{u}' \cdot \boldsymbol{u}') - \bar{\mu}}{(\boldsymbol{u} \cdot \boldsymbol{u})} = \frac{2L(\boldsymbol{u})\boldsymbol{u}' \cdot L(\boldsymbol{u})\boldsymbol{u}'}{R^{*2}} - \frac{\bar{\mu}}{R^*}$$

$$\boldsymbol{u}'' = \frac{\bar{h}}{2}\boldsymbol{u} + L^T(\boldsymbol{u})\bar{\bar{B}} L(\boldsymbol{u})\boldsymbol{u}' + \frac{(\boldsymbol{u} \cdot \boldsymbol{u})}{2} L^T(\boldsymbol{u})\boldsymbol{F}^{**} \tag{27}$$

Unlike the restricted circular case, where the singularity in $\bar{h}$ at $R^* = 0$ is easily removed by using a form for $\bar{h}$ written in terms of the Jacobi constant C_J, here $\bar{h}$ is now obtained through numerical integration of an appropriate differential equation in nonsingular form,

$$\bar{h}' = (\boldsymbol{F}^{**}, \boldsymbol{R}^{*\prime}) = 2[\boldsymbol{u}', L^T(\boldsymbol{u})\boldsymbol{F}^{**}], \qquad \bar{h}' = 2\boldsymbol{u}'^T L^T(\boldsymbol{u})\boldsymbol{F}^{**}$$

$$\frac{d\bar{h}}{d\tau} = \bar{h}' = 2(u_1' u_2' u_3' u_4') \begin{pmatrix} u_1 & u_2 & u_3 & u_4 \\ -u_2 & u_1 & u_4 & -u_3 \\ -u_3 & -u_4 & u_1 & u_2 \\ u_4 & -u_3 & u_2 & -u_1 \end{pmatrix} \begin{pmatrix} F_1^{**} \\ F_2^{**} \\ F_3^{**} \\ 0 \end{pmatrix} \tag{28}$$

In Eq. (28), the notation[12] $(\boldsymbol{x}, \boldsymbol{y}) = \boldsymbol{x}^T \boldsymbol{y}$ for the scalar product is used. Backward integration of the vector differential Eq. (27) is carried out with respect to $\tau' = -\tau$, such that Eq. (27) is equivalent to the system of eight first-order differential equations

$$u_1' = v_1 \tag{29}$$

$$u_2' = v_2 \tag{30}$$

$$u_3' = v_3 \tag{31}$$

$$u_4' = v_4 \tag{32}$$

$$v_1' = (\bar{h}/2)u_1 - 2b\left[\left(u_1^2 + u_2^2\right)v_2 + (u_2 u_3 - u_1 u_4)v_3 - (u_1 u_3 + u_2 u_4)v_4\right] + \tfrac{1}{2}\left(u_1^2 + u_2^2 + u_3^2 + u_4^2\right) \times \left(u_1 F_1^{**} + u_2 F_2^{**} + u_3 F_3^{**}\right) \tag{33}$$

$$v_2' = (\bar{h}/2)u_2 - 2b\left[-\left(u_1^2 + u_2^2\right)v_1 + (u_2 u_4 + u_1 u_3)v_3 + (u_2 u_3 - u_1 u_4)v_4\right] + \tfrac{1}{2}\left(u_1^2 + u_2^2 + u_3^2 + u_4^2\right) \times \left(-u_2 F_1^{**} + u_1 F_2^{**} + u_4 F_3^{**}\right) \tag{34}$$

$$v_3' = (\bar{h}/2)u_3 - 2b\left[(u_1 u_4 - u_2 u_3)v_1 - (u_1 u_3 + u_2 u_4)v_2 + \left(u_3^2 + u_4^2\right)v_4\right] + \tfrac{1}{2}\left(u_1^2 + u_2^2 + u_3^2 + u_4^2\right) \times \left(-u_3 F_1^{**} - u_4 F_2^{**} + u_1 F_3^{**}\right) \tag{35}$$

$$v_4' = (\bar{h}/2)u_4 - 2b\left[(u_2 u_4 + u_1 u_3)v_1 + (u_1 u_4 - u_2 u_3)v_2 - \left(u_3^2 + u_4^2\right)v_3\right] + \tfrac{1}{2}\left(u_1^2 + u_2^2 + u_3^2 + u_4^2\right) \times \left(u_4 F_1^{**} - u_3 F_2^{**} + u_2 F_3^{**}\right) \tag{36}$$

The prime in Eqs. (29–36) stands for derivation with respect to τ', and $\bar{h}$ is obtained from Eq. (28) without any change in sign because $d\bar{h}/d\tau'$ has the same form as $d\bar{h}/d\tau$ in Eq. (28), where the prime stands for derivation with respect to τ. The form of $d\bar{h}/d\tau'$ is identical to $d\bar{h}/d\tau$ because $du_1/d\tau = u_1'$, u_2', u_3', and u_4', which are with respect to τ in Eq. (28), will change to $-du_1/d\tau'$, $-u_2'$, $-u_3'$, and $-u_4'$ in $d\bar{h}/d\tau'$ in Eq. (37):

$$\frac{d\bar{h}}{d\tau'} = 2\left[u_1'\left(u_1 F_1^{**} + u_2 F_2^{**} + u_3 F_3^{**}\right) + u_2'\left(-u_2 F_1^{**} + u_1 F_2^{**} + u_4 F_3^{**}\right) + u_3'\left(-u_3 F_1^{**} - u_4 F_2^{**} + u_1 F_3^{**}\right) + u_4'\left(u_4 F_1^{**} - u_3 F_2^{**} + u_2 F_3^{**}\right)\right] \tag{37}$$

The physical time t is obtained from

$$\frac{dt}{d\tau'} = -\left(u_1^2 + u_2^2 + u_3^2 + u_4^2\right) \tag{38}$$

Thus, the system of 10 differential equations, namely, Eqs. (29–38), is integrated simultaneously without any singularity at $R^* = 0$.

Except for the case where $\bar{h}$ is initialized at $R^* = 0$, the Earth's center, the system of 10 differential equations is then truly free of any singularity, even during integration through $R^* = 0$.

Numerical Results

Figure 3 shows the sun-centered Earth geometry with $\hat{X}_e$, $\hat{Y}_e$, and $\hat{Z}_e$ inertial and $\hat{r}$, $\hat{\theta}$, and $\hat{h}$ and x, y, and z rotating and attached, respectively, to the Earth and to L_1. The rotation from $\hat{r}$, $\hat{\theta}$, and $\hat{h}$ to the ecliptic is given by

$$\begin{pmatrix}\hat{X}_e\\ \hat{Y}_e\\ \hat{Z}_e\end{pmatrix} = \begin{pmatrix} c_{\Omega\oplus}c_{\theta\oplus} - s_{\Omega\oplus}c_{i\oplus}s_{\theta\oplus} & -c_{\Omega\oplus}s_{\theta\oplus} - s_{\Omega\oplus}c_{i\oplus}c_{\theta\oplus} & s_{\Omega\oplus}s_{i\oplus}\\ s_{\Omega\oplus}c_{\theta\oplus} + c_{\Omega\oplus}c_{i\oplus}s_{\theta\oplus} & -s_{\Omega\oplus}s_{\theta\oplus} + c_{\Omega\oplus}c_{i\oplus}c_{\theta\oplus} & -c_{\Omega\oplus}s_{i\oplus}\\ s_{i\oplus}s_{\theta\oplus} & s_{i\oplus}c_{\theta\oplus} & c_{i\oplus}\end{pmatrix}\begin{pmatrix}\hat{r}\\ \hat{\theta}\\ \hat{h}\end{pmatrix}$$

$$= \begin{pmatrix} A_\oplus & C_\oplus & G_\oplus\\ B_\oplus & D_\oplus & H_\oplus\\ E_\oplus & F_\oplus & K_\oplus\end{pmatrix}\begin{pmatrix}\hat{r}\\ \hat{\theta}\\ \hat{h}\end{pmatrix} = R_{\Omega\oplus i\oplus\theta\oplus}\begin{pmatrix}\hat{r}\\ \hat{\theta}\\ \hat{h}\end{pmatrix} \tag{39}$$

The ecliptic position and velocity components are obtained from $\boldsymbol{r} = \boldsymbol{R} + \boldsymbol{\rho}'$ and $\boldsymbol{v} = \dot{\boldsymbol{R}} + \dot{\boldsymbol{\rho}}'$ with

$$\boldsymbol{\rho}' = \left(\rho'_{\hat{X}_e} \quad \rho'_{\hat{Y}_e} \quad \rho'_{\hat{Z}_e}\right)^T, \qquad \dot{\boldsymbol{\rho}}' = \dot{\boldsymbol{\rho}}'_I + \boldsymbol{\omega}\times\boldsymbol{\rho}'$$

and where

$$\dot{\boldsymbol{\rho}}'_I = (\dot{x}'_I \quad \dot{y}'_I \quad \dot{z}'_I)^T, \qquad \boldsymbol{\omega} = R_{\Omega\oplus i\oplus\theta\oplus}\boldsymbol{\omega}_R$$

$$\boldsymbol{\omega}_R = (0 \quad 0 \quad \dot{\theta}_\oplus)^T, \qquad \dot{\theta}_\oplus = \frac{(1-e^2)^{\frac{1}{2}}}{(1-ec_E)^2}$$

as in Eq. (4), due to the similarity of the various elliptic orbits as discussed earlier. Also,

$$\rho'_{\hat{X}_e} = A_\oplus x' + C_\oplus y' + G_\oplus z', \qquad \rho'_{\hat{Y}_e} = B_\oplus x' + D_\oplus y' + H_\oplus z'$$

$$\rho'_{\hat{Z}_e} = E_\oplus x' + F_\oplus y' + K_\oplus z', \qquad \boldsymbol{R} = R(A_\oplus \quad B_\oplus \quad E_\oplus)^T$$

with $R = (1 - ec_E)$ in nondimensional form such that

$$X_e = RA_\oplus + \rho'_{\hat{X}_e}, \qquad Y_e = RB_\oplus + \rho'_{\hat{Y}_e}, \qquad Z_e = RE_\oplus + \rho'_{\hat{Z}_e}$$

$$\dot{X}_e = -[(\mu_\odot + \mu_\oplus)/h]\left[c_{\Omega\oplus}\left(s_{\theta\oplus} + es_{\omega\oplus}\right) + s_{\Omega\oplus}\left(c_{\theta\oplus} + ec_{\omega\oplus}\right)c_{i\oplus}\right]$$
$$+ (A_\oplus\dot{x}' + C_\oplus\dot{y}' + G_\oplus\dot{z}') - \dot{\theta}_\oplus\left(c_{\Omega\oplus}s_{i\oplus}\rho'_{\hat{Z}_e} + c_{i\oplus}\rho'_{\hat{Y}_e}\right)$$

$$\dot{Y}_e = -[(\mu_\odot + \mu_\oplus)/h]\left[s_{\Omega\oplus}\left(s_{\theta\oplus} + es_{\omega\oplus}\right) - c_{\Omega\oplus}\left(c_{\theta\oplus} + ec_{\omega\oplus}\right)c_{i\oplus}\right]$$
$$+ (B_\oplus\dot{x}' + D_\oplus\dot{y}' + H_\oplus\dot{z}') - \dot{\theta}_\oplus\left(s_{\Omega\oplus}s_{i\oplus}\rho'_{\hat{Z}_e} - c_{i\oplus}\rho'_{\hat{X}_e}\right)$$

$$\dot{Z}_e = -[(\mu_\odot + \mu_\oplus)/h]\left(c_{\theta\oplus} + ec_{\omega\oplus}\right)s_{i\oplus} + (E_\oplus\dot{x}' + F_\oplus\dot{y}' + K_\oplus\dot{z}')$$
$$+ \dot{\theta}_\oplus\left(s_{\Omega\oplus}s_{i\oplus}\rho'_{\hat{Y}_e} + c_{\Omega\oplus}s_{i\oplus}\rho'_{\hat{X}_e}\right) \tag{40}$$

The first term in each of the $\dot{X}_e$, $\dot{Y}_e$, and $\dot{Z}_e$ expressions represents the contribution from $\dot{\boldsymbol{R}}$ with $\mu_\odot$ and $\mu_\oplus$ standing for the gravity constant of the sun and the Earth and with $\mu_\odot + \mu_\oplus = 1$ and $h = (1 - e^2)^{1/2}$ due to the normalization. Here, h is the angular momentum of the primaries and has the dimensional form $\sqrt{[G(m_1 + m_2)a(1 - e^2)]}$, whereas $(\mu_\odot + \mu_\oplus)$ has the form

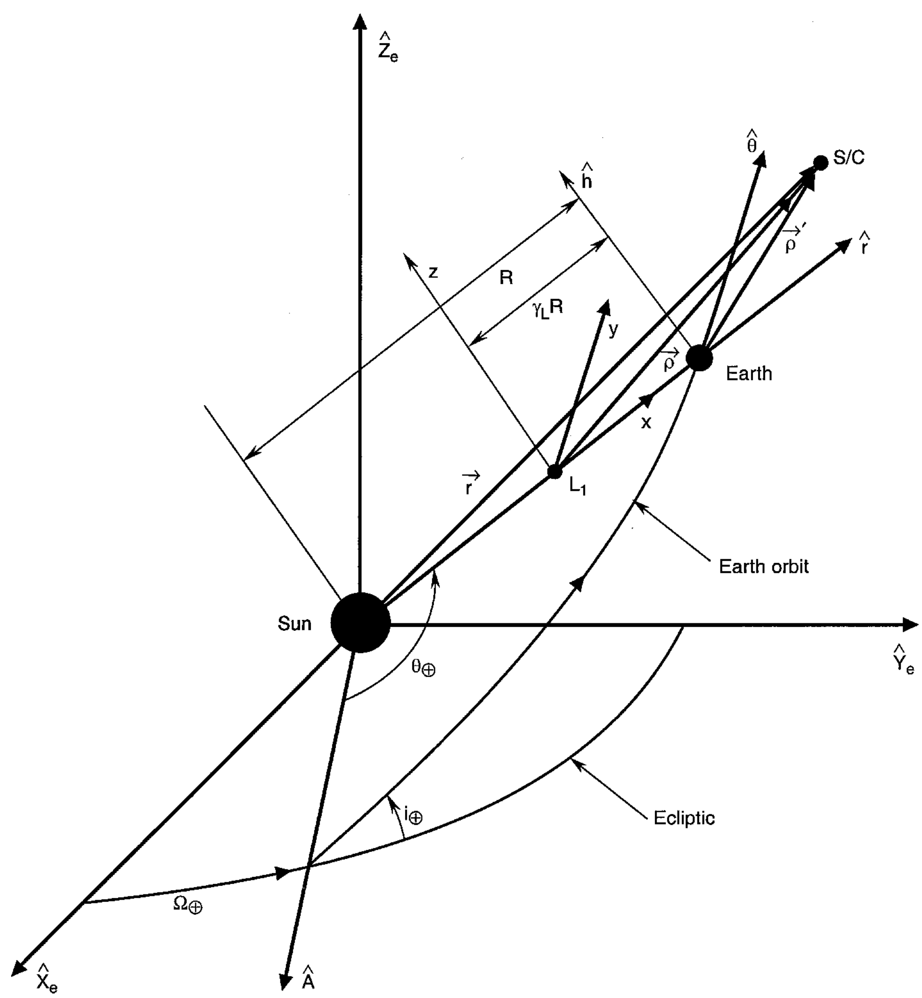

Fig. 3 Earth geometry in sun-centered system.

$G(m_1+m_2)$ before its normalization. Finally,

$$\begin{pmatrix}\dot{x}'_I\\ \dot{y}'_I\\ \dot{z}'_I\end{pmatrix}=\begin{pmatrix}A_\oplus & C_\oplus & G_\oplus\\ B_\oplus & D_\oplus & H_\oplus\\ E_\oplus & F_\oplus & K_\oplus\end{pmatrix}\begin{pmatrix}\dot{x}'\\ \dot{y}'\\ \dot{z}'\end{pmatrix},\qquad \begin{pmatrix}\dot{x}'\\ \dot{y}'\\ \dot{z}'\end{pmatrix}=\begin{pmatrix}\dot{x}-\gamma_L\dot{R}\\ \dot{y}\\ \dot{z}\end{pmatrix} \tag{41}$$

The relative velocity components $\dot{x}'_I$, $\dot{y}'_I$, and $\dot{z}'_I$ are observed in the $\hat{r}$, $\hat{\theta}$, and $\hat{h}$ frame, but measured along the ecliptic axes $\hat{X}_e$, $\hat{Y}_e$, and $\hat{Z}_e$. Also, $\dot{x}'$ and $\dot{x}$ differ by the quantity $\gamma_L\dot{R}$, which is variable as a function of the eccentric anomaly E because $\dot{R}=es_E\dot{E}$ with $\dot{E}=1/(1-ec_E)$. Also, $x'=x-\gamma_L R$, $y'=y$, and $z'=z$, such that the spacecraft position and velocity components X'_e, Y'_e, and Z'_e and $\dot{X}'_e$, $\dot{Y}'_e$, and $\dot{Z}'_e$ in the inertial Earth-centered ecliptic system, whose axes $\hat{X}'_e$, $\hat{Y}'_e$, and $\hat{Z}'_e$ are parallel to $\hat{X}_e$, $\hat{Y}_e$, and $\hat{Z}_e$, are now given by Eqs. (40), without the first term in each of these equations, or, in practice, without the $\boldsymbol{R}$ and $\dot{\boldsymbol{R}}$ contributing terms. The state vector is rotated to the equatorial Earth-centered system $\hat{X}_{\text{eq}}$, $\hat{Y}_{\text{eq}}$, and $\hat{Z}_{\text{eq}}$, using

$$(X_{\text{eq}}\quad Y_{\text{eq}}\quad Z_{\text{eq}})^T=T^{-1}(X'_e\quad Y'_e\quad Z'_e)^T \tag{42}$$

$$(\dot{X}_{\text{eq}}\quad \dot{Y}_{\text{eq}}\quad \dot{Z}_{\text{eq}})^T=T^{-1}(\dot{X}'_e\quad \dot{Y}'_e\quad \dot{Z}'_e)^T \tag{43}$$

where

$$T=\begin{pmatrix}1 & 0 & 0\\ 0 & c_\varepsilon & s_\varepsilon\\ 0 & -s_\varepsilon & c_\varepsilon\end{pmatrix}$$

and where ε is the obliquity of the ecliptic. Finally, the components x', y', z', $\dot{x}'$, $\dot{y}'$, and $\dot{z}'$ are readily obtained from

$$\begin{pmatrix}x'\\ y'\\ z'\end{pmatrix}=\begin{pmatrix}A_\oplus & B_\oplus & E_\oplus\\ C_\oplus & D_\oplus & F_\oplus\\ G_\oplus & H_\oplus & K_\oplus\end{pmatrix}\begin{pmatrix}X'_e\\ Y'_e\\ Z'_e\end{pmatrix} \tag{44}$$

$$\begin{pmatrix}\dot{x}'\\ \dot{y}'\\ \dot{z}'\end{pmatrix}=\begin{pmatrix}A_\oplus & B_\oplus & E_\oplus\\ C_\oplus & D_\oplus & F_\oplus\\ G_\oplus & H_\oplus & K_\oplus\end{pmatrix}\left[\begin{pmatrix}\dot{X}'_e\\ \dot{Y}'_e\\ \dot{Z}'_e\end{pmatrix}+\dot{\theta}_\oplus\begin{pmatrix}-H_\oplus\rho'_{\hat{Z}_E}+K_\oplus\rho'_{\hat{Y}_E}\\ G_\oplus\rho'_{\hat{Z}_E}-K_\oplus\rho'_{\hat{X}_E}\\ -G_\oplus\rho'_{\hat{Y}_E}+H_\oplus\rho'_{\hat{X}_E}\end{pmatrix}\right] \tag{45}$$

$$(x\quad y\quad z\quad \dot{x}\quad \dot{y}\quad \dot{z})^T=(x'+\gamma_L\, y'\, z'\, \dot{x}'+\gamma_L\dot{R}\, y'\, z')^T \tag{46}$$

When t_{ref} stands for a reference time when the primaries are at their respective perigees, with $(M_\odot)_{t_{\text{ref}}}=0$, and a transfer time t_{f_o} is guessed, as well as the velocity changes at t_{f_o} on a given halo orbit, at a given location on that orbit, the mean anomaly of the sun at t_{f_o} is evaluated from $(M_\odot)_{t_{f_o}}=(M_\odot)_{t_{\text{ref}}}-n_E(t_{\text{ref}}-t_{f_o})$, followed by the eccentric anomaly $(E_\odot)_{t_{f_o}}$ obtained from the Kepler equation $M=E-es_E$, and, thereby, the true anomaly $(\theta^*_\odot)t_{f_o}$ from $\tan(\theta^*/2)=[(1+e)/(1-e)]^{1/2}\tan(E/2)$. The angular positions of the sun and the Earth at t_{f_o} are obtained from $(\theta_\odot)_{t_{f_o}}=(\theta^*_\odot)_{t_{f_o}}+\omega_\odot$ and $(\theta_\oplus)_{t_{f_o}}=(\theta_\odot)_{t_{f_o}}+\pi$, such that $(\theta^*_\oplus)_{t_{f_o}}=(\theta_\oplus)_{t_{f_o}}-\omega_\oplus$. Here, $\omega_\odot$ and $\omega_\oplus$ are the arguments of perigee of the orbits of the sun and the Earth, respectively. They are selected as π and 0 in the following calculations. The eccentric anomaly of the Earth $(E_\oplus)_{t_{f_o}}$ is obtained from

$$\tan^{-1}\left[s_{(E_\oplus)_{t_{f_o}}}/c_{(E_\oplus)_{t_{f_o}}}\right]$$

using the well-known relationships

$$c_E=\frac{e+c_{\theta^*}}{1+ec_{\theta^*}},\qquad s_E=\frac{(1-e^2)^{\frac{1}{2}}s_{\theta^*}}{1+ec_{\theta^*}}$$

The rates

$$(\dot{R})_{t_{f_o}}=\frac{es_{(E_\oplus)_{t_{f_o}}}}{1-ec_{(E_\oplus)_{t_{f_o}}}},\qquad (\dot{\theta}_\oplus)_{t_{f_o}}=\frac{(1-e^2)^{\frac{1}{2}}}{(1-ec_{(E_\oplus)_{t_{f_o}}})^2}$$

are also evaluated at the guessed time t_{f_o}, and, by the use of $\Omega_\oplus=0$ and $i_\oplus=0$ in our calculations for the Eulerian angles of the Earth's orbit, the elements $A_\oplus,\ldots,K_\oplus$ of the rotation matrix are computed at t_{f_o}. With

$$(R)_{t_{f_o}}=1-ec_{(E_\oplus)_{t_{f_o}}}$$

with $e=0.0167217$ throughout,

$$x'=x_o-\gamma_L(R)_{t_{f_o}},\qquad y'=y_o,\qquad z'=y_o$$

the components of $\boldsymbol{\rho}'$, are computed from the given L_1-centered initial position components x_o, y_o, and z_o on the given halo orbit of interest, as well as

$$\dot{x}'=\dot{x}_o-\gamma_L(\dot{R})_{t_{f_o}},\qquad \dot{y}'=\dot{y}_o,\qquad \dot{z}'=\dot{z}_o$$

from its L_1-centered velocity components. The quantities X'_e, Y'_e, and Z'_e and $\dot{X}'_e$, $\dot{Y}'_e$, and $\dot{Z}'_e$ are now readily evaluated from the knowledge of $\rho'_{\hat{X}_e}$, $\rho'_{\hat{Y}_e}$, and $\rho'_{\hat{Z}_e}$ and $\dot{x}'_I$, $\dot{y}'_I$, and $\dot{z}'_I$ in Eq. (41), such that the equatorial quantities $X_{\text{eq}},\ldots,\dot{Z}_{\text{eq}}$ in Eqs. (42) and (43) are also evaluated using $\varepsilon=i_s=23.440$ deg. Thus, a set of Earth-centered osculating orbital elements can also be produced. The values of x_o, y_o, z_o, $\dot{x}_o$, $\dot{y}_o$, and $\dot{z}_o$ are set as x, y, z, $\dot{x}$, $\dot{y}$, and $\dot{z}$, from which the corresponding values of u_1, u_2, u_3, u_4, u'_1, u'_2, u'_3, and u'_4, as well as $\bar{h}$, are initialized before the integration. Thus,

$$x^*=x-\gamma_L(R)_{t_{f_o}},\qquad \dot{x}^*=\dot{x}-\gamma_L(\dot{R})_{t_{f_o}}$$

$$r=\left(x^{*^2}+y^2+z^2\right)^{\frac{1}{2}}$$

If $x^*>0$, then $u_4=(\frac{1}{2}x^*)^{1/2}$, u_1 is computed from $u_1^2+u_4^2=\frac{1}{2}(r+x^*)$, and

$$u_2=\frac{yu_1+zu_4}{r+x^*},\qquad u_3=\frac{zu_1-yu_4}{r+x^*}$$

If $x^*<0$, then $u_3=(-\frac{1}{2}x^*)^{1/2}$, after which u_2 is computed from $u_2^2+u_3^2=\frac{1}{2}(r-x^*)$, and, finally,

$$u_1=\frac{yu_2+zu_3}{r-x^*},\qquad u_4=\frac{zu_2-yu_3}{r-x^*}$$

Also, the velocities are obtained from

$$u'_1=-\tfrac{1}{2}\left(u_1\dot{x}^*+u_2\dot{y}+u_3\dot{z}\right),\qquad u'_2=-\tfrac{1}{2}\left(-u_2\dot{x}^*+u_1\dot{y}+u_4\dot{z}\right)$$

$$u'_3=-\tfrac{1}{2}\left(-u_3\dot{x}^*-u_4\dot{y}+u_1\dot{z}\right),\qquad u'_4=-\tfrac{1}{2}\left(u_4\dot{x}^*-u_3\dot{y}+u_2\dot{z}\right)$$

and $\bar{h}$ from

$$\bar{h}=\frac{2(\boldsymbol{u}'\cdot\boldsymbol{u}')-\bar{\mu}}{(\boldsymbol{u}\cdot\boldsymbol{u})}$$

where $\boldsymbol{u}\cdot\boldsymbol{u}=R^*$. As τ' increases, starting from $\tau'=0$, the physical time t decreases from its initialized guessed value at t_{f_o},

$$M_\oplus(t)=(M_\oplus)_{t_{f_o}}-n_E\left(t_{f_o}-t\right)$$

is evaluated at each t, $(E_\oplus)_t$ is evaluated from Kepler's equation such that $(\theta^*_\oplus)_t$ and $(\theta_\oplus)_t$ are also computed for the current calculation of

$$(R)_t=1-ec_{(E_\oplus)_t},\qquad (\dot{R})_t=\frac{es_{(E_\oplus)_t}}{\left[1-ec_{(E_\oplus)_t}\right]}$$

$$(\dot{\theta}_\oplus)_t=\frac{(1-e^2)^{\frac{1}{2}}}{\left[1-ec_{(E_\oplus)_t}\right]^2}$$

The values of $A_\oplus,\ldots,K_\oplus$, $x'=x-\gamma_L(R)_t$, y', and z'; $\rho'_{\hat{X}_e}$, $\rho'_{\hat{Y}_e}$, and $\rho'_{\hat{Z}_e}$; $\dot{x}'=\dot{x}-\gamma_L(\dot{R})_t$, $\dot{y}'$, and $\dot{z}'$; $\dot{x}'_I$, $\dot{y}'_I$, and $\dot{z}'_I$; X'_e, Y'_e, and Z'_e; and $\dot{X}'_e$, $\dot{Y}'_e$, and $\dot{Z}'_e$ are then evaluated during each integration step as the system of 10 differential equations are integrated, such that the equatorial components $X_{\text{eq}},\ldots,\dot{Z}_{\text{eq}}$ that lead to the evaluation

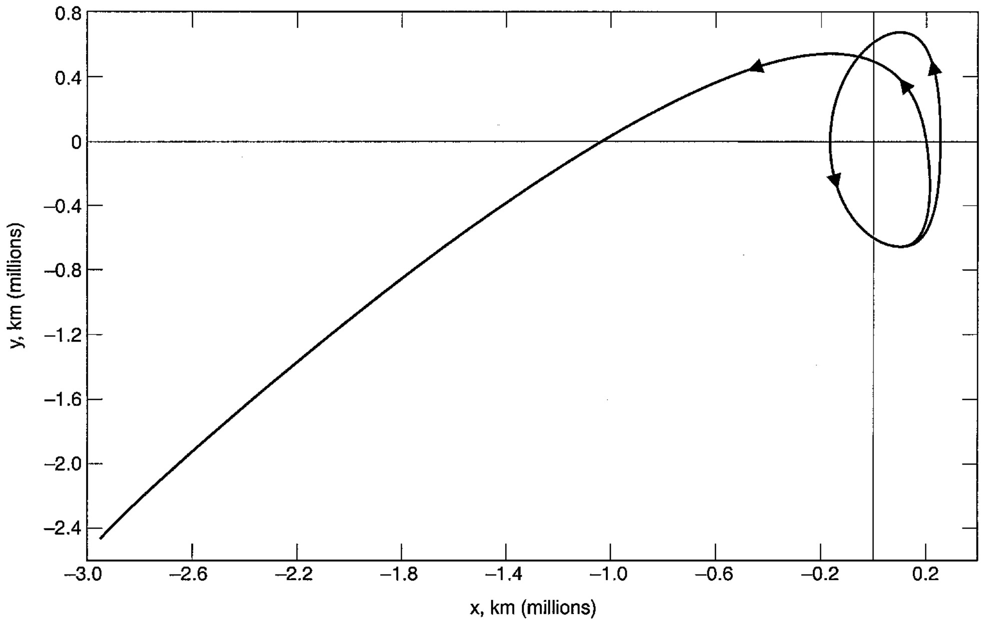

Fig. 4 Backward path of halo orbit integrated by using elliptic equations.

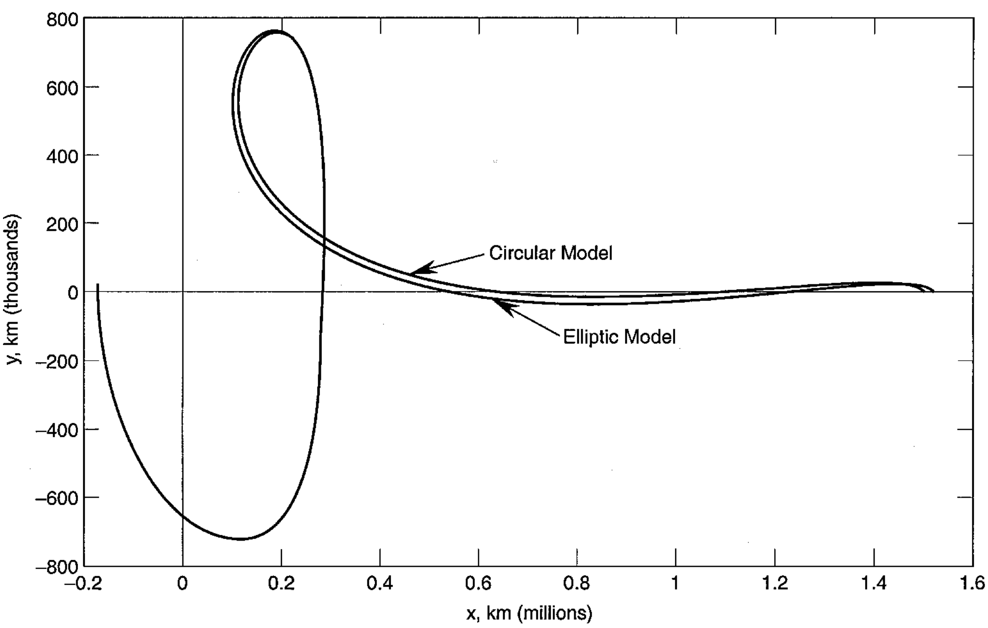

Fig. 5 Transfer trajectories' x–y traces in the circular and elliptic problems.

of the equivalent set of Earth-centered osculating orbit elements are also computed. The integration is stopped on the $\boldsymbol{r} \cdot \boldsymbol{v} = 0$ condition, and the achieved values of r_s, the radius of closest approach to the Earth, as well as the argument of perigee ω, are then slowly driven to their target values of r_T and ω_T by searching on the $\Delta\dot{x}$ and $\Delta\dot{y}$ components at the starting point. The value of t_{f_o} is also adjusted until the backward integration also ends at or near time zero. The coefficients b, c, d, and k, which are functions of $(E_\oplus)_t$, and which are needed in the differential equations that are being integrated, as well as in the components of the forcing function $\boldsymbol{F}^{**}$, are updated at each integration step after updating $(R)_t$, $(\dot{R})_t$, as well as $x = x^* + \gamma_L(R)_t$, from $x^* = u_1^2 - u_2^2 - u_3^2 + u_4^2$ in terms of the u variables, and $y = 2u_1u_2 - 2u_3u_4$ and $z = 2u_1u_3 + 2u_2u_4$. The example that follows uses the initial conditions $x = -1.713125475 \times 10^5$ km, $y = 2.476726461 \times 10^4$ km, $z = 1.418553080 \times 10^5$ km, $\dot{x} = 4.538772391 \times 10^{-3}$ km/s, $\dot{y} = 2.672159950 \times 10^{-1}$ km/s, and $\dot{z} = -1.667431943 \times 10^{-3}$ km/s, which correspond to the 90-day point on an L_1-centered halo orbit computed within the assumption of the restricted circular problem. By the use of $\mu = 3.040357143 \times 10^{-6}$ and $\gamma_L = 1.0011 \times 10^{-2}$ throughout, as well as $t_{\text{ref}} = 9.977358094 \times 10^8$ s, these initial conditions are traced backward with $e = 0$ and 0.0167217, respectively. Figure 4 shows that the halo orbit closes into itself in the first instance and skips out of its periodic path in the second or in the elliptic assumption. A search is carried out next, to match an altitude h_T of 185 km at closest approach to the Earth, as well as an $\omega_T = 170$ deg using a guess for $\Delta\dot{x} = -2$ m/s, $\Delta\dot{y} = -2$ m/s, and $t_{f_o} = 0.17 \times 10^8$ s. A feasible solution converging on $h_{\text{alt}} = 184.964$ km, $\omega = 172.887$ deg, with $\Delta\dot{x} = 6.140394$ m/s and $\Delta\dot{y} = 22.56431$ m/s is found that requires a transfer time of 201.459874750 days. The insertion ΔV of 23.384 m/s is higher than for the circular solution of Ref. 16, which required $\Delta\dot{x} = 5.952283$ m/s and $\Delta\dot{y} = 18.634630$ m/s, or a ΔV of 19.562 m/s and a shorter transfer time of 198.524198 days. Figure 5 shows the x–y trace of this transfer trajectory, as well as the trace of the transfer obtained with $e = 0$, that is, the circular problem depicted in Ref. 16 that also integrates backward from the same L_1-relative initial conditions.

Conclusions

A set of regularized differential equations that describes the exact motion of a spacecraft flying in three-dimensional space, in the gravitational field of a binary system where the two primaries are in their respective elliptic orbits, is derived. The method of backward integration is used to integrate the nonsingular state vector cast in the u language, starting from the halo orbit or from any other selected point in space to the vicinity of the Earth. The initial conditions are searched until the target parameters of choice near the Earth are fully achieved. The use of this set of regularized variables bypasses the need to consider constrained optimization software that are more difficult to manipulate than their simpler unconstrained versions, resulting in effective robustness in quickly generating a desired transfer path from the Earth to any selected point in space. It is also shown that the elliptic model used here provides accurate results, which are quite impossible with the circular model solution.

The present regularized system of equations can be used in conjunction with the invariant manifold approach for trajectory generation to and from periodic orbits or their nearby orbits, especially when transferring from the Earth or when the flight path makes repeated close passes to the Earth. It can also be used to globalize the stable manifolds more accurately, as it can for the system model in differential correction schemes used to solve general two-point boundary-value problems by way of continuation methods.

Acknowledgment

This work was supported by the U.S. Air Force Space and Missile Systems Center under Contract F04701-93-C-0094.

References

[1]Farquhar, R. W., "The Control and Use of Libration-Point Satellites," NASA TR R-346, 1970.

[2]Szebehely, V., *Theory of Orbits*, Academic Press, New York, 1967, pp. 587–602.

[3]Moulton, F. R., *An Introduction to Celestial Mechanics*, 2nd rev. ed., Dover, New York, 1970, pp. 277–319.

[4]Plummer, H. C., *An Introductory Treatise on Dynamical Astronomy*, Dover, New York, 1960, pp. 236–252.

[5]Brouwer, D., and Clemence, G. M., *Methods of Celestial Mechanics*, Academic Press, New York, 1961, pp. 253–272.

[6]Richardson, D. L., "Analytic Construction of Periodic Orbits About the Colinear Points," *Celestial Mechanics*, Vol. 22, 1980, pp. 241–253.

[7]Pernicka, H. J., "The Numerical Determination of Nominal Libration Point Trajectories and Development of a Stationkeeping Strategy," Ph.D. Dissertation, School of Aeronautics and Astronautics, Purdue Univ., West Lafayette, IN, May 1990.

[8]Hiday, L. A., "Optimal Transfers Between Libration-Point Orbits in the Elliptic Restricted Three-Body Problem," Ph.D. Dissertation, School of Aeronautics and Astronautics, Purdue Univ., West Lafayette, IN, July 1992.

[9]Levi-Civita, T., "Sur la Résolution Qualitative du Problème Restreint des Trois Corps," *Operemathematiche*, Vol. 2, 1956, pp. 99–144.

[10]Kustaanheimo, P., "Spinor Regularization of the Kepler Motion," *Annales Universitatis Turkuensis Series AI*, Vol. 73, 1964, pp. 1–7.

[11]Kustaanheimo, P., and Stiefel, E., "Perturbation Theory of Kepler Motion Based on Spinor Regularization," *Journal für Mathematik*, Vol. 218, 1965, pp. 204–219.

[12]Stiefel, E. L., and Scheifele, G., *Linear and Regular Celestial Mechanics*, Springer-Verlag, New York, 1971, pp. 18–33.

[13]Howell, K. C., and Breakwell, J. V., "Almost Rectilinear Halo Orbits," *Celestial Mechanics*, Vol. 32, 1984, pp. 24–52.

[14]Mains, D. L., "Transfer Trajectories from Earth Parking Orbits to L_1 Halo Orbits," M.S. Thesis, School of Aeronautics and Astronautics, Purdue Univ., West Lafayette, IN, May 1993.

[15]Kechichian, J. A., "The Efficient Computation of Transfer Trajectories Between Earth Orbit and L_1 Halo Orbit Within the Framework of the Sun–Earth Restricted Circular Three Body Problem," American Astronautical Society, Paper AAS-00-174, Jan. 2000.

[16]Kechichian, J. A., "Transfer Trajectories from Low Earth Orbit to a Large L_1-Centered Class I Halo Orbit in the Sun–Earth Circular Problem," American Astronautical Society, Paper AAS 00-252, March 2000.

[17]Howell, K. C., Barden, B. T., and Lo, M. W., "Application of Dynamical Systems Theory to Trajectory Design for a Libration Point Mission," *Journal of the Astronautical Sciences*, Vol. 45, No. 2, 1997, pp. 161–178.

[18]Koon, W. S., Lo, M. W., Masdemont, J. E., and Ross, S. D., "Shoot the Moon," American Astronautical Society, Paper AAS 00-166, Jan. 2000.

[19]Gómez, G., and Masdemont, J., "Some Zero Cost Transfers Between Libration Point Orbits," American Astronautical Society, Paper AAS 00-177, Jan. 2000.

[20]Howell, K. C., Mains, D. L., and Barden, B. T., "Transfer Trajectories from Earth Parking Orbits to Sun–Earth Halo Orbits," American Astronautical Society, Paper AAS 94-160, Feb. 1994.

[21]Gómez, G., Llibre, J., Martínez, R., and Simó, C., "Dynamics and Mission Design Near Libration Points, Vol. I, Fundamentals: The Case of Collinear Libration Points," Vol. 2, World Scientific Monograph Series in Mathematics, World Scientific, Singapore, Republic of Singapore, 2001, pp. 143–150.

[22]Barden, B. T., "Using Stable Manifolds to Generate Transfers in the Circular Restricted Problem of Three Bodies," M.S. Thesis, School of Aeronautics and Astronautics, Purdue Univ., West Lafayette, IN, Dec. 1994.

[23]Bettis, D. G., and Szebehely, V., "Treatment of Close Approaches in the Numerical Integration of the Gravitational Problem of N Bodies," *Astrophysics and Space Science*, Vol. 14, 1971, pp. 133–150.

[24]Ocampo, C., "Trajectory Optimization for Distant Earth Satellites and Satellite Constellations," Ph.D. Dissertation, Dept. of Aerospace Engineering Sciences, Univ. of Colorado, Boulder, CO, 1996.

[25]Ocampo, C. A., and Rosborough, G. W., "Transfer Trajectories for Distant Retrograde Orbiters of the Earth," American Astronautical Society, Paper AAS 93-180, Feb. 1993.

[26]Kahaner, D., Moler, C., and Nash, S., *Numerical Methods and Software*, Prentice–Hall, Englewood Cliffs, NJ, 1989, pp. 347–384.